ISSN 0020-1685, Inorganic Materials, 2015, Vol. 51, No. 5, pp. 436–440. © Pleiades Publishing, Ltd., 2015.
Original Russian Text © S.A. Kuznetsova, A.A. Pichugina, V.V. Kozik, 2015, published in Neorganicheskie Materialy, 2015, Vol. 51, No. 5, pp. 490–495.

Microwave-Assisted Hydrothermal Process for the Preparation of SnO from an Ammoniacal $Sn_6O_4(OH)_4$ Suspension

S. A. Kuznetsova, A. A. Pichugina, and V. V. Kozik

National Research Tomsk State University, pr. Lenina 36, Tomsk, 634050 Russia

e-mail: alina.com9@mail.ru

Received September 30, 2014

Abstract—SnO powder with a specific surface area of 2 m^2/g has been prepared by microwave-assisted hydrothermal processing of an ammoniacal $Sn_6O_4(OH)_4$ suspension. We have examined the effect of pressure rise rate in a reaction mixture on the surface morphology and photocatalytic activity of SnO. Raising the pressure has been shown to reduce the SnO synthesis time, without influencing the surface morphology of SnO or its photocatalytic activity for methyl orange photodegradation.

DOI: 10.1134/S002016851504007X

INTRODUCTION

The synthesis of nanomaterials with controlled surface morphology and a preferred orientation of crystal growth faces is a key issue in nanotechnology development [1, 2]. This has recently led most researchers to study the effect of synthesis conditions on the surface structure and morphology of materials, including SnO [3–5]. This oxide has found wide application in laser sensors, as an anode material for lithium ion batteries, and as a photocatalyst [6–9]. Among known SnO preparation techniques, hydrothermal and microwave-assisted hydrothermal processes allow one to produce structures with various orientations of crystal growth faces and various surface morphologies [10–13]. Hydrothermal processing offers a number of advantages: high growth rate of large crystals, high nucleation rate, relatively low synthesis temperature, structural uniformity of the resulting materials, etc. [14, 15]. Unfortunately, there is currently very little data on the effect of pressure in a reaction mixture on SnO morphology and the amount of active surface centers contributing to changes in functional properties.

In connection with this, the purpose of this work was to study the effect of pressure in the preparation of SnO under microwave-assisted hydrothermal synthesis conditions from an ammoniacal $Sn_6O_4(OH)_4$ suspension on its surface morphology and photocatalytic activity.

EXPERIMENTAL

An ammoniacal $Sn_6O_4(OH)_4$ suspension was prepared by dissolving metallic tin in concentrated hydrochloric acid, followed by Sn^{2+} precipitation with an excess of 25% aqueous ammonia [9]. The resultant tin(II) oxyhydroxide suspension was placed in a Teflon autoclave and subjected to microwave-assisted hydrothermal processing (MAHP) in an MS-6 Vol'ta system at a microwave power of 539 W for 5 min. The pressure in the autoclave was raised at a rate of 3.3 kPa/s. The precipitate was separated by centrifugation, repeatedly washed with distilled water, and dried at 90°C.

The SnO formation process was followed using thermal analysis of the solid phase ($Sn_6O_4(OH)_4$) in the suspension under an argon atmosphere with a Netzsch STA 449 system at a heating rate of 10°C/min in the temperature range 25–1000°C. The activation energy for all stages of the decomposition process was evaluated using the Erofeev–Kolmogorov equation [16].

The phase composition of the final synthesis products was determined by X-ray diffraction on a Rigaku Miniflex 600 diffractometer (CuK_α radiation, 10°–90° (2θ), scan step of 0.02°, scan rate of 5°/min). Diffraction peaks were indexed using JCPDS PDF data. The specific surface area of the SnO samples was determined by BET analysis of low-temperature nitrogen adsorption isotherms obtained using a TriStar II automatic gas adsorption analyzer. Surface morphologies were examined by scanning electron microscopy on a Hitachi TM3000 equipped with a QUANTAX energy dispersive spectrometer system. IR spectra of the samples were measured in the frequency range 1000–4000 cm^{-1} on an Agilent Technologies Cary 600 Series FTIR spectrophotometer.

The photocatalytic activity of the synthesized SnO powders was assessed for methyl orange azo dye photodegradation as a model reaction. The SnO powder was mixed with a methyl orange solution in a quartz beaker. To reach sorption–desorption equilibrium, the mixture was stirred in the dark. Next, the reaction mixture was placed under an I_2 excimer ultraviolet lamp with $\lambda = 342$ nm and exposed to UV radiation for 60 min with constant stirring. Every 10 min, we took

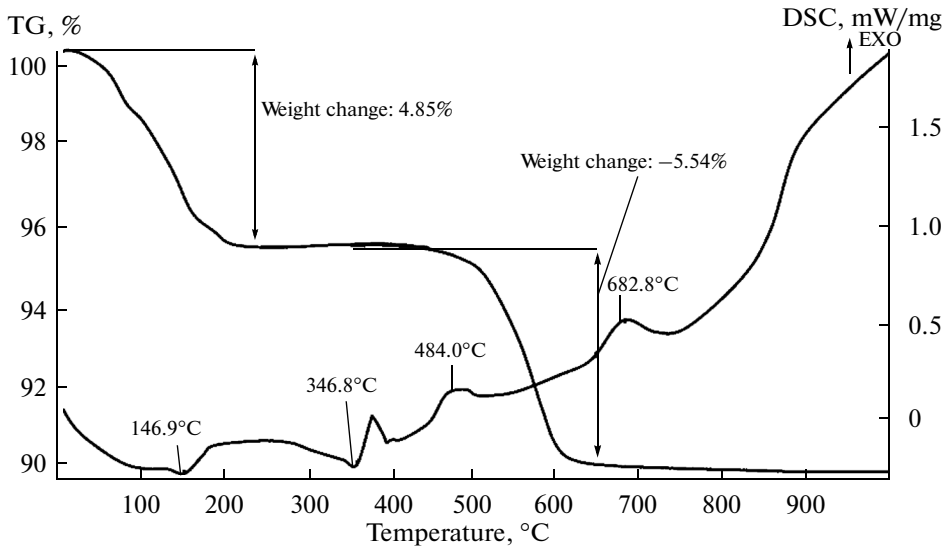

Fig. 1. Thermal analysis results for $Sn_6O_4(OH)_4$ decomposition in an inert atmosphere.

an aliquot, which was centrifuged to separate the precipitate, and then the absorbance of the mother liquor was measured. The methyl orange concentration was determined spectrophotometrically on a PE-5400 UF spectrophotometer from the height of the absorption peak at $\lambda = 461$ nm. The absolute accuracy limits in the transmission measurements were ±0.5%.

The composition of the methyl orange photodecomposition products after UV exposure was determined using a Surveyor high-performance liquid chromatography (HPLC) system equipped with an autosampler and an LCQ Advantage MAX mass spectrometric detector. Components were separated in a HyperSil Gold column packed with a reversed phase sorbent (C_{18}) grafted on silica gel with a particle size of 5 μm. The eluents used were a formic acid solution (0.1 wt %) and acetonitrile (100 wt %). The eluent flow rate was 0.5 L/min.

RESULTS AND DISCUSSION

According to thermal analysis data, the solid phase of the $Sn_6O_4(OH)_4$ suspension in an argon atmosphere decomposes in two steps (Fig. 1). The first step, in the temperature range 25–230°C, is accompanied by an endothermic peak at $t = 146.9$°C. The low activation energy for this process (42.49 kJ/mol) may point to the removal of the adsorbed water and ammonia molecules remaining after $Sn_6O_4(OH)_4$ drying. X-ray diffraction data indicate that the composition of the intermediate product of this step is $Sn_6O_4(OH)_4$. According to the Erofeev–Kolmogorov equation and curve, the second step of the decomposition process, in the temperature range 250–650°C, involves endothermic (346.8°C) and exothermic (484.0°C) processes. The activation energy for this step is considerably higher, 178.12 kJ/mol, pointing to the dissociation of chemically bound OH groups in the compound.

Thus, the $Sn_6O_4(OH)_4$ decomposition process at a heating rate of 10°C/min, resulting in SnO formation at a temperature of 600°C in 60 min, can be represented by the following scheme:

$$Sn_6O_4(OH)_4(NH_{3(ads)} \cdot H_2O_{(ads)}) \xrightarrow{-NH_{ads},\ -H_2O_{ads}} Sn_6O_4(OH)_4 \xrightarrow{-2H_2O} SnO.$$

As shown earlier [9], the formation of tin(II) oxide with high photocatalytic activity from an ammoniacal tin(II) oxyhydroxide suspension requires microwave processing for at least 15 min at a microwave power of 539 W. The SnO sample obtained under such conditions, even though having a small specific surface area of 3 m^2/g, showed high catalytic activity for methyl orange azo dye photodegradation, which can be understood in terms of pore shape, volume, and size [9]. As follows from curves *1* in Fig. 2, the SnO sample has a mesoporous structure nonuniform in pore shape, with a pore volume of 8×10^{-4} $cm^3/(g\ nm)$ and a broad pore size (diameter) distribution, from 5 to 20 nm.

The present results demonstrate that the SnO synthesis time can be reduced by performing microwave synthesis under pressure. According to X-ray diffraction data, microwave-assisted hydrothermal processing for just 5 min at a pressure rise rate of 3.3 kPa/s in the autoclave and a microwave power of 539 W yielded blue black powder, which was identified as tetragonal SnO with lattice parameters $a = b = 3.804$ nm and $c = 4.837$ nm and a crystallite size of 57 nm in the [002] crystal growth direction and 49 nm in the [101] direction (Fig. 3).

This oxide is close in pore volume and pore size to the SnO sample prepared by microwave processing for 15 min and also has a small specific surface area (2 m^2/g). According to the hysteresis loop in its nitro-

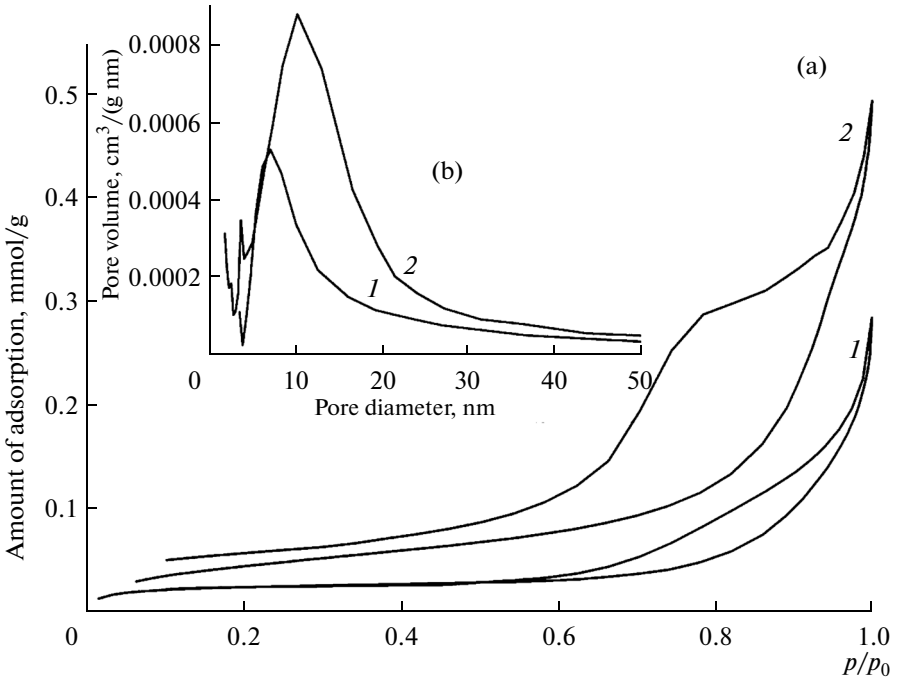

Fig. 2. (a) Nitrogen adsorption–desorption isotherms and (b) differential pore size distribution curves for the SnO samples prepared (*1*) by microwave processing for 15 min and (*2*) by MAHP for 5 min.

gen adsorption–desorption isotherm, the oxide is a mesoporous adsorbent nonuniform in pore shape (Fig. 2a, curve *1*). It is seen from the differential pore size distribution curve of this sample (Fig. 2b, curve *1*) that its structure contains pores of volume 6×10^{-4} $cm^3/(g\ nm)$, ranging in diameter from 5 to 20 nm.

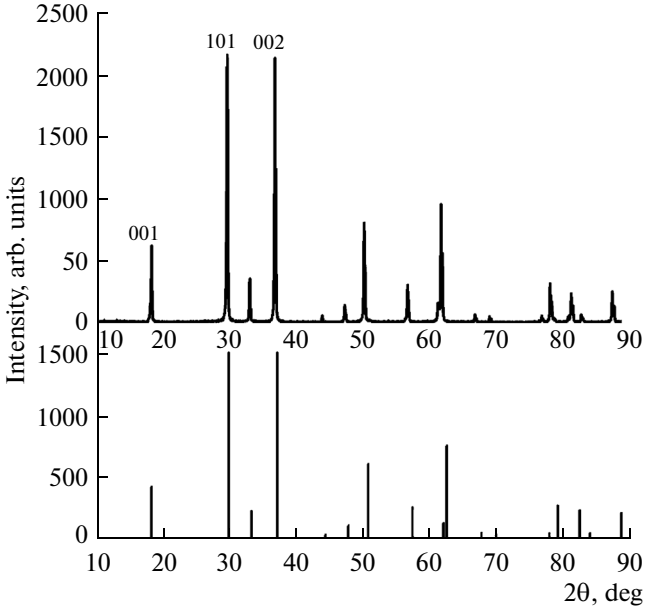

Fig. 3. X-ray diffraction pattern of the SnO sample prepared by MAHP for 5 min.

According to scanning electron microscopy results, the SnO sample consists of platelike particles in the form of irregularly shaped fragments, among which agglomerates 5–6 μm in size and large particles, up to 15 μm in size, prevail (Fig. 4).

IR spectroscopy results indicate that, after storage in air, the surface of the above SnO sample was covered with water and oxygen molecules adsorbed from the air. The absorption bands in the range 2350–3450 cm^{-1} are due to adsorbed water molecules (stretching ν and bending δ modes of OH groups). The absorption bands in the range 1620–1650 cm^{-1} correspond to

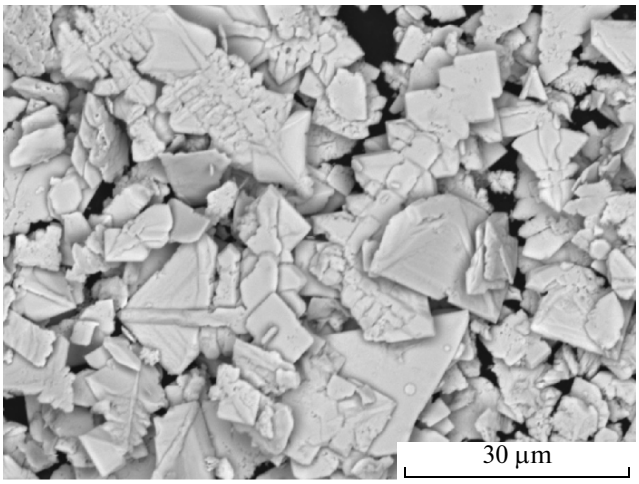

Fig. 4. Micrograph of the SnO sample prepared by MAHP for 5 min.

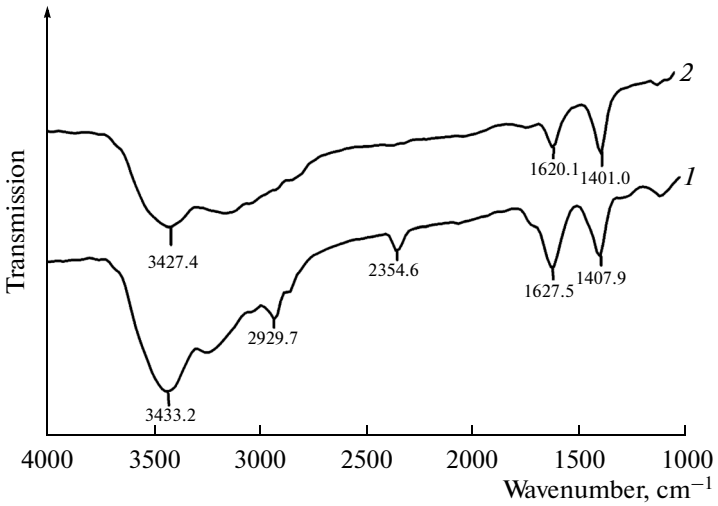

Fig. 5. IR spectra of the SnO powder prepared in 5 min (*1*) before and (*2*) after heat treatment.

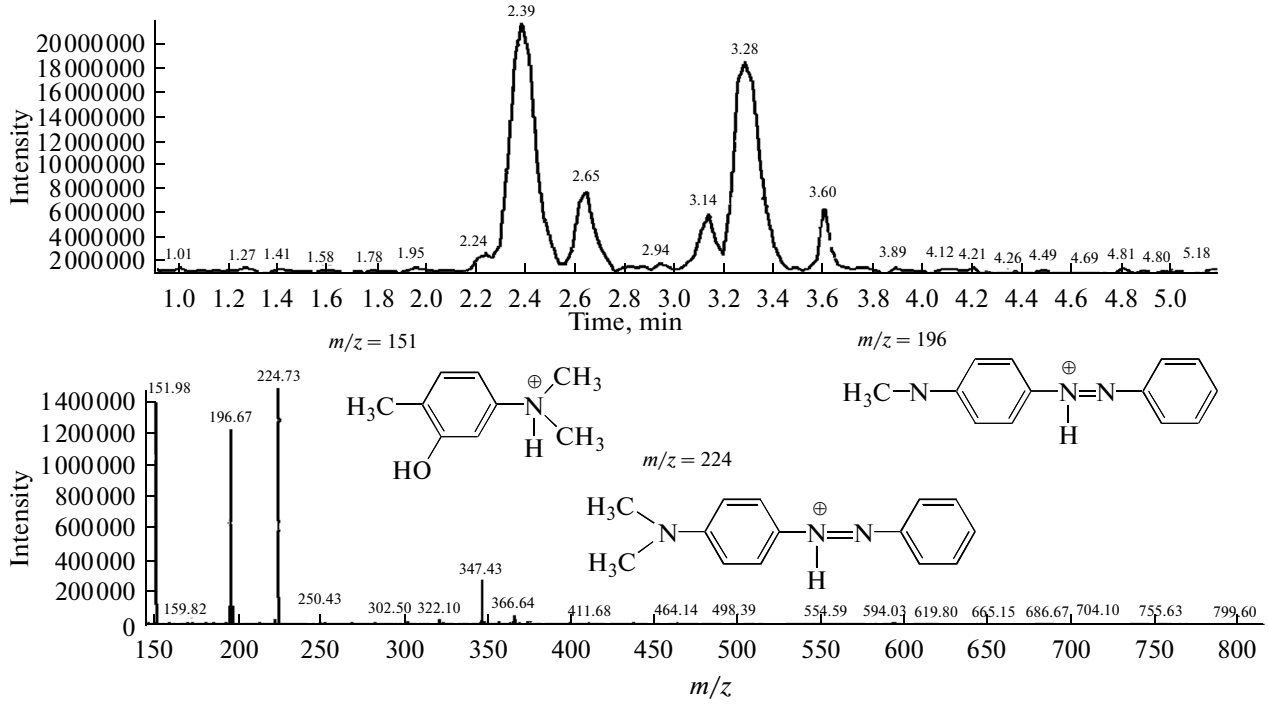

Fig. 6. HPLC/mass spectrometry data for positively charged species after UV-induced methyl orange decomposition.

adsorbed oxygen molecules, with coordinatively unsaturated Sn atoms on the oxide surface. The spectrum of this sample contains an absorption band at 1407.4 cm^{-1}. According to data in the literature [17–19], this band is attributable to bonds with adsorbed H_2O and O_2 molecules (Fig. 5, spectrum *1*). That this absorption corresponds to physisorbed molecules is evidenced by the fact that heat treatment of the samples at $t = 100$°C changes its intensity in the IR spectra, to the extent that it disappears (Fig. 5, spectrum *2*).

Photocatalytic activity assessment showed that the sample under consideration had a considerable sorption capacity for methyl orange. After stirring the suspension in the dark for 1 h, its surface sorbed up to 35 wt % of the methyl orange. Subsequent UV exposure for 60 min led to methyl orange decomposition (95%). Liquid chromatography/mass spectrometry data indicated that, after the photocatalytic processing of methyl orange in the presence of the SnO sample, the major methyl orange decomposition products were positively charged species with molecular weights of 224, 196, and 151. Their tentative compositions are presented in Fig. 6.

Our findings indicate that, all other factors being the same, the pressure during the microwave-assisted hydrothermal synthesis of SnO from an ammoniacal $Sn_6O_4(OH)_4$ suspension influences the synthesis time.

CONCLUSIONS

The present results demonstrate that raising the pressure during the microwave synthesis of SnO from an ammoniacal $Sn_6O_4(OH)_4$ suspension reduces the synthesis time. At a pressure rise rate of 3.3 kPa/s in the autoclave and a microwave power of 539 W, the SnO synthesis time decreases by a factor of 3. It is worth noting that the SnO thus prepared compares well in photocatalytic properties to the oxide prepared by microwave processing and is similar in surface morphology [9].

ACKNOWLEDGMENTS

This work was supported by the RF Ministry of Education and Science, state research target no. 1432.

REFERENCES

1. Wang, X., Yang, Y.J., and Jao, J.N., Controlled synthesis of multi-shelled transition metal oxide hollow structures through one-pot solution route, *Chin. Chem. Lett.,* 2013, vol. 24, pp. 1–6.
2. Hassan Farooq, M., Riaz Hassian, Linge Zhang, Aslam, I., Tanveer, M., Shah, M.W., and Zubair Iqbal, Fabrication, characterization and magnetic properties of Mn-doped SnO nanostructures via hydrothermal method, *Mater. Lett.*, 2014, vol. 131, pp. 350–353.
3. Zubair Iqbal, M., Fengping Wang, Ting Feng, Hailei Zhao, Yasir Rafique, M., Rafi-ud-Din, Hassan Farooq, Qurat u lain Javed, and DilFaraz Khan, Facile synthesis of self-assembled SnO nano-square sheets and hydrogen absorption characteristics, *Mater. Res. Bull.*, 2012, vol. 47, pp. 3902–3907.
4. Sheng-Chang Wang, Ray Kuang Chiang, and Din-jie Hu, Morphological and phase control of tin oxide single-crystals synthesized by dissolution and recrystallization of bulk SnO powders, *J. Ceram. Soc.*, 2011, vol. 31, pp. 2447–2451.
5. Ying Liang, Huiwen Zheng, and Bin Fang, Synthesis and characterization of SnO with controlled flower like microstructures, *Mater. Lett.*, 2013, vol. 108, pp. 235–238.
6. Hu, Y., Xu, K., Kong, L., Jiang, H., Zhang, L., and Li, C., Flame synthesis of single crystalline SnO nanoplateles lithium-ion batteries, *Chem. Eng. J.*, 2013, vol. 242, pp. 220–225.
7. Uchiyama, H., Hosono, E., Honma, I., Zhou, H.S., and Imai, H., A nanoscale meshed electrode of single-crystalline SnO for lithium-ion rechargeable batteries, *Electrochem. Commun.*, 2008, vol. 10, pp. 52–55.
8. Yang, J., Takeda, Y., Imanishi, N., Xie, T.Y., and Yamamoto, O., Morphology modification and irreversibility compensation for SnO anodes, *J. Power Source*, 2001, vols. 97–98, pp. 216–218.
9. Kuznetsova, S.A., Pichugina, A.A., and Kozik, V.V., Microwave synthesis of a photocatalytically active SnO-based material, *Inorg. Mater.*, 2014, vol. 50, no. 4, pp. 387–391.
10. Jeong Ho Shin, Jae Yong Song, Young Heon Kim, and Hyum Min Park, Low temperature and self-catalytic growth of tetragonal SnO nanobranch, *Mater. Lett.*, 2010, vol. 64, pp. 1120–1122.
11. Kangkang Men, Jiajia Ning, Quanqin Dai, Dongmei Li, Bingbing Liu, Yu, W.W., and Bo Zou, Synthesis of SnO crystals with shape control via ligands interaction and limited ligand protection, *Colloids Surf., A*, 2010, vol. 363, pp. 30–34.
12. Giefers, H., Parsch, F., and Wortmann, G., Structural study of SnO at high pressure, *Phys. B* (Amsterdam, Neth.), 2006, vol. 373, pp. 76–81.
13. Zubair Iqbal, M., Fengping Wang, Rafi-ud-Din, Yasir Rafique, M., Quarat-ul-ain Javed, Asad Ullah, and Hongmei Qiu, Synthesis of novel clinapinacoid structure of stannous oxide and hydrogen absorption characteristics, *Mater. Lett.*, 2012, vol. 78, pp. 50–53.
14. Balakhonov, S.V., Ivanov, V.K., Baranchikov, A.V., and Churagulov, B.R., A comparative analysis of the physicochemical properties of vanadium-oxide-based nanomaterials prepared by hydrothermal and microwave-assisted hydrothermal processes, *Nanosist.: Fiz., Khim., Mat.*, 2012, vol. 3, no. 4, pp. 66–74.
15. Byrappa, K. and Yoshimura, M., *Handbook of Hydrothermal Technology*, New York: William Andrew, 2001.
16. Fialko, M.B., *Neizotermicheskaya kinetika v termicheskom analize* (Nonisothermal Kinetics in Thermal Analysis), Tomsk: Tomsk. Gos. Univ., 1981.
17. Kazitsina, L.A. and Kupletskaya, N.B., *Primenenie UF-, IK- i YaMR-spektroskopii v organicheskoi khimii* (Application of UV, IR, and NMR Spectroscopies in Organic Chemistry), Moscow: Vysshaya Shkola, 1971.
18. Davydov, A.A., *IK-spektroskopiya v khimii poverkhnosti okislov* (IR Spectroscopy and Chemistry of Oxide Surfaces), Novosibirsk: Nauka, 1984.
19. Nakamoto, K., *Infrared and Raman Spectra of Inorganic and Coordination Compounds*, New York: Wiley, 1986.

Translated by O. Tsarev